Microelectrode investigation of the lithium redox behavior in plasticized polymer electrolytes

Xian-Ming Wang, Makoto Iyoda, Tatsuo Nishina *, Isamu Uchida

Department of Applied Chemistry, Graduate School of Engineering, Tohoku University, Aramaki-Aoba, Aoba-ku, Sendai 980-77, Japan

Abstract

The lithium redox behavior in plasticized polymer electrolytes has been studied by microelectrode technique with the advantage in decreasing the iR effect of solution resistance. PAN (polyacrylonitrile)-, PVdF (poly(vinylidene fluoride))- and PVC (poly(vinyl chloride))-based plasticized electrolytes showed ionic conductivities ranging from 10^{-4} to 10^{-3} S/cm at ambient temperature. By applying high scan rate ($-V/s$), the aggravating effect of the electrolyte decomposition with freshly deposited lithium was suppressed, and the reliable kinetic parameters of the lithium deposition/dissolution and the diffusion coefficient of lithium ion were evaluated for PAN- and PVdF-based electrolytes. The obtained diffusion coefficient for the PAN-based electrolyte was 1.50×10^{-6} cm^2/s at 21 °C, indicating that the plasticized polymer electrolytes behaved as a pure organic solution of plasticizer. © 1997 Published by Elsevier Science S.A.

Keywords: Plasticized polymer electrolytes; Conductivity; Lithium redox behavior; Electrode kinetics

1. Introduction

Considerable effort has been paid to the development of the polymer electrolytes with the high ionic conductivity due to their potential application in solid-state rechargeable lithium batteries. The polymer electrolytes, possessing conductivities around 10^{-3} S/cm, which are similar to those of organic solutions, are obtained via either manipulation of the electrolyte structure [1] or addition of the plasticizers, such as propylene carbonate and ethylene carbonate (PC + EC), to the polymer hosts [2]. On the other hand, much less attention has been paid to the redox reaction of Li in polymer electrolytes; it is important to understand the fundamentals of the interfacial behavior of Li because it is a well-known limitation factor of the cycle life of rechargeable Li batteries [3].

A problem inherent in the study of the Li electrode reaction is the decomposition reaction of nonaqueous elelctrolytes with the freshly deposited Li, which addresses the aggravating effect on the analytical results [4]. In addition, the data are also distorted by the uncompensated iR drops due to the high resistance of the nonaqueous electrolytes. These problems can be avoided by the use of microelectrodes because of their dramatic improvement in decreased sensitivity of the effect of solution resistivity and increased temporal resolution

even at high scan rate [5]. These advantages of the microelectrode technique have been elucidated in our previous study on the Li deposition/dissolution reaction in organic solutions [6]. As well, the convincing reasons were given by the other groups to show interesting prospects in the utilization of microelectrodes to study the Li electrode reaction [7–10].

As the extended work of the kinetic study on Li deposition/dissolution in organic solutions, we turned our attention to poly(acrylonitrile) (PAN), poly(vinylidene fluoride) (PVdF) and poly(vinyl chloride) PVC-based polymer electrolytes containing propylene carbonate and ethyl carbonate (PC + EC) as plasticizers in this work. To achieve this aim, the microelectrode technology was applied.

2. Experimental

PAN (mol. wt. 1.3×10^5), PVdF (mol. wt. 7.7×10^4), PVC (mol. wt. 6.9×10^4) and LiClO$_4$/PC + EC solution (water content < 20 ppm) were received from Mitsubishi Institution of Technology, Kureha Chemical, Wako Chemical and Mitsubishi Chemical, respectively. The plasticized polymer electrolytes were prepared by adding polymers and LiClO$_4$/PC + EC to the solvent such as PC + EC or THF, solidifying and pressing into thin film in a argon glove box as described by Abraham et al. [2], Alamgir and Abraham
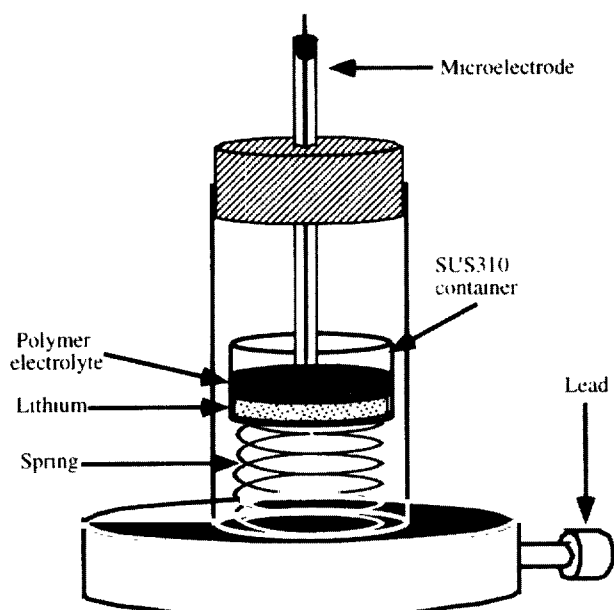
* Corresponding author

Fig 1 Schematic of the electrochemical cell assembly for polymer electrolytes

Fig. 2. Arrhenius plot of the conductivity of 8LiClO$_4$/33PC + 38EC/21PAN (mol%) electrolyte (0.24 mm in thickness).

Table 1
Conductivity of various electrolytes at ambient temperature

Electrolyte (mol%)	$\sigma \times 10^3$ (S/cm)
8LiClO$_4$/38EC + 33PC/21PAN	1.66 (23 °C)
4LiClO$_4$/40EC + 35PC/21PVC	0.29 (25 °C)
3LiClO$_4$/38EC + 33PC/26PVdF	3.10 (25 °C)
7LiClO$_4$/51EC + 42PC (1 M)	6.30 (25 °C)

[11] and Tsuchida et al. [12]. Apparently, the dimensional stability of PVC was higher than that of PAN and PVdF.

Fig. 1 shows the schematic of the cell assembly. A spring was used to keep good electrical contact of the polymer electrolyte with the electrode. The electrochemical measurement was carried out in a two-electrode configuration. A Pt (diameter 30 μm) microelectrode was constructed by sealing a Pt wire into Pyrex glass tube. An Li foil served as the counter electrode. In addition, the conductivity of the polymer electrolytes was determined from a.c. impedance measurements. Conductivity measurements were performed in a specially designed cell with stainless-stell disk electrodes (0.2 cm^2).

The electrochemical measurement was performed by a computer-controlled elctrochemical system (Cypress Systems, Model CS-1090) and LCR meter (Hewlett Packard, Model 4332A). The water content in the solution was detected by the Karl–Fischer titration (Mitsubishi, Model CA-06). An Al-sealed box was utilized to reduce the electrical noise.

3. Results and discussion

3.1. Conductivity

Fig. 2 shows the Arrhenius plot of the conductivity of the PAN-based polymer. The conductivity was 1.6×10^{-3} S/cm at 23 °C, and a discontinuity point was observed at ~ 30 °C. This type of discontinuity has been reported by Yang et al. [13] for plasticized poly(ethylene oxide) (PEO) electrolyte at 45 °C, and attributed to the existence of a low melting phase in the system [13]. Furthermore, it was found that the conductivity increased with increasing the content of the plasticizer.
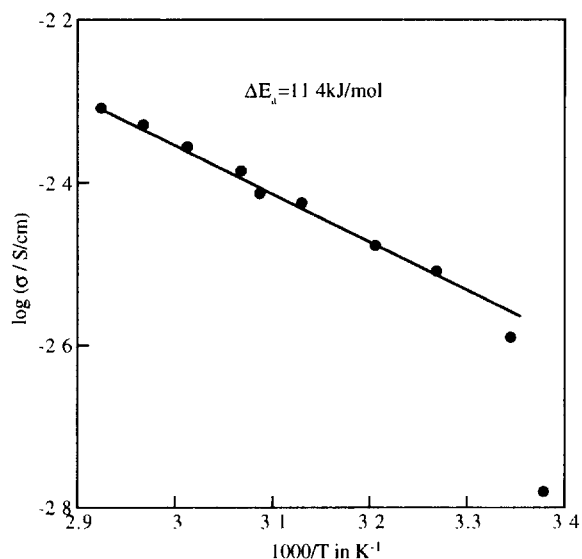
In the similar way, we measured the conductivity of PVC- and PVdF-based plasticized polymer electrolytes, and the results are summarized in Table 1 together with the conductivity value of 1 M LiClO$_4$/PC + EC solution. It was clear that these plasticized polymers possessed high conductivity as same as the 1 M LiClO$_4$/PC + EC solution at ambient temperature. Furthermore, it was found that the temperature-dependent curves of conductivity did not show any discontinuity below 60 °C for PVdF- and PVC-based electrolytes.

3.2. Electrolyte stability

Fig. 3 shows the effect of the reversed potential on cyclic voltammetry at a Pt microelectrode in 8LiClO$_4$/33PC + 38EC/21PAN (mol%) electrolyte at 1 V/s. At the reversed potential of − 1.2 V, an abruptly increasing cathodic current was observed after Li deposition, indicating the occurrence of the electrolyte decomposition reaction with freshly deposited Li as the case of pure organic solutions [6]. While the electrolyte decomposition occurred at a more negative potential than − 1.0 V, only Li deposition was observed when the reversed potential was more positive than − 0.8 V. It is clear that the electrolyte decomposition with the freshly deposited Li was suppressed due to a short exposure duration of Li surface in the electrolyte by applying the rapid scan rate and the positive reversed potential. This enables us to evaluate
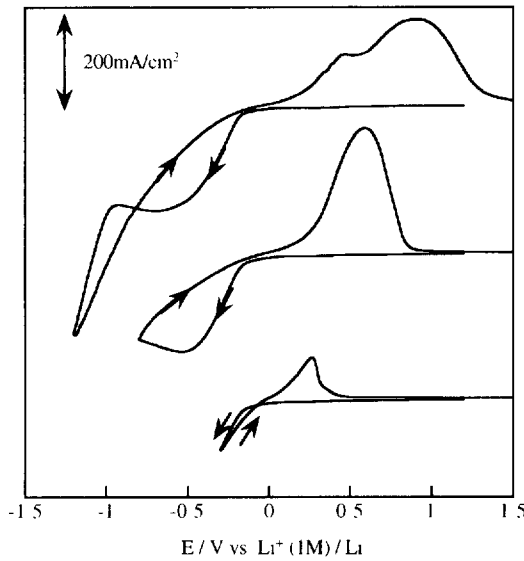
Fig. 3. Effect of the reversed potential on cyclic voltammery at the Pt microelectrode (diameter 30 μm) in 8LiClO₄/33PC+38EC/21PAN (mol%) electrolyte at 21 °C; scan rate: 1 V/s
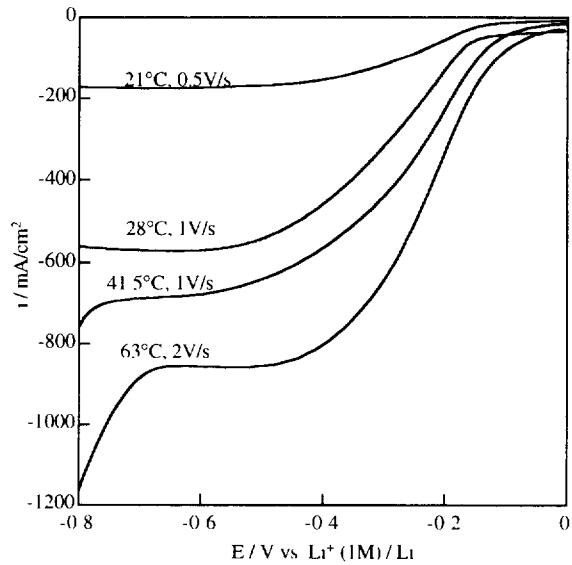

Fig. 4. Effect of the temperature on the cyclic voltammograms of Li deposition at the Pt microelectrode (diameter 30 μm) in 8LiClO₄/33PC+38EC/21PAN (mol%) electrolyte.

the kinetic parameters without the aggravating effect of electrolyte decomposition.

3.3. Diffusion of lithium ion

Fig. 4 shows cyclic voltammograms of a Pt microelectrode (diameter 30 μm) in PAN-based electrolyte as a function of temperature. The potential was initially set to +1.2 V, at which no appreciable current was observed, then scanned to −0.8 V and reversed to +1.5 V. It was found that the faster scan rate was needed to obtain the well-defined sigmoid curves at the higher temperature, because the decomposition of the electrolyte became easier with increasing temperature. According to the microelectrode theory, the limiting current density was independent of the scan rate, as expressed in the following equation, the different scan rate gave no influence on the calculated result of the diffusion coefficient

$$i_L = -\frac{4nFDC}{r\pi(1-t_+)} \tag{1}$$

where i_L is the limiting current density, n the electron number, F the Faraday constant, C the bulk concentration of Li ion, D the diffusion coefficient, r the radius of the Pt microdisk electrode, and t_+ the transference number of the Li ion. By supposing t_+ to be 0.3 and independent of the temperature,

the diffusion coefficients were calculated from the limiting current density, and the results are summarized in Table 2 together with the diffusion coefficients in 1 M LiClO₄/PC+EC solution for comparison.

Fig. 5 shows the Arrhenius plot of the diffusion coefficient. A steplike change was observed at 30 °C, which is similar to the temperature dependence of the conductivity as shown in Fig. 2. The activation energy for the diffusion coefficient also agreed well with that of conductivity. These may be attributed to the proportional relation of diffusion coefficient and conductivity [14].

The diffusion coefficients of the Li ion were also evaluated in PAN- and PVdF-based electrolyte and summarized in Table 2. It was found that the diffusion coefficients in these two plasticized polymer electrolytes were identical to that in 1 M LiClO₄/PC+EC solution, indicating that the plasticized polymer electrolytes behaved most like as an LiClO₄/PC+EC solution [15].

3.4. Kinetic parameters for lithium deposition/dissolution

Fig. 6 shows cyclic voltammograms for the Pt microelectrode in PAN-based electrolyte at 23 °C at 1 V/s, where the potential was reversed at −0.4 V to maintain the Li deposition/dissolution process in charge-transfer control. The

Table 2
Diffusion coefficient of Li ion in 1 M LiClO₄/PC+EC solution, 8LiClO₄ (1 M)/33PC+38EC/21PAN (mol%) and 3LiClO₄ (0 26 M)/33PC+38EC/26PVdF (mol%) electrolytes with assuming the transfer number of lithium ion as $t_+ = 0.3$

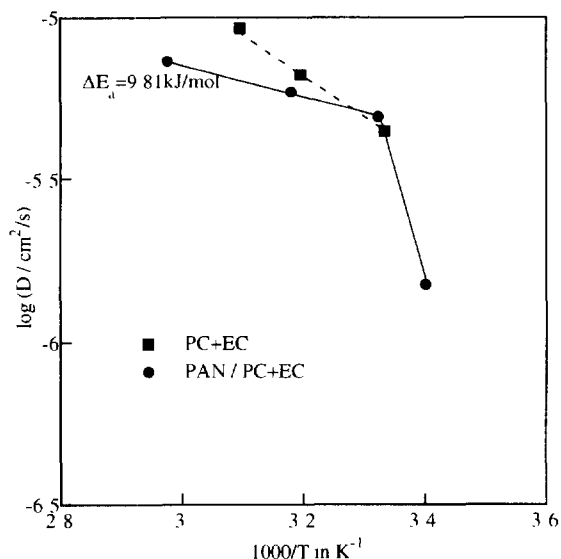|	PC+EC			PAN/PC+EC				PVdF/PC+EC			
	27 °C	40 °C	50 °C	21 °C	28 °C	41.5 °C	63 °C	20 °C	26 °C	38 °C	70 °C
$D \times 10^6$ cm²/s	4.42	6.66	9 27	1.50	4 90	5.89	7.38	1.34	1 48	1.83	3.16
ΔE_a (kJ/mol)	24.2			9 81				14.3			

Fig 5. Arrhenius plot of the diffusion coefficients of the Li ion in 1 M LiClO₄/PC + EC solution and 8LiClO₄ (1 M)/33PC + 38EC/21PAN (mol%) electrolyte
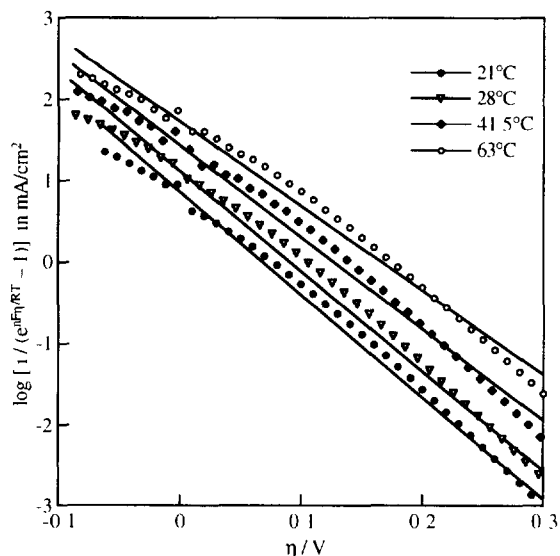

Fig. 7. Allen–Hickling plots of Li deposition/dissolution in 8LiClO₄ (1 M)/33PC + 38EC/21PAN (mol%) electrolyte
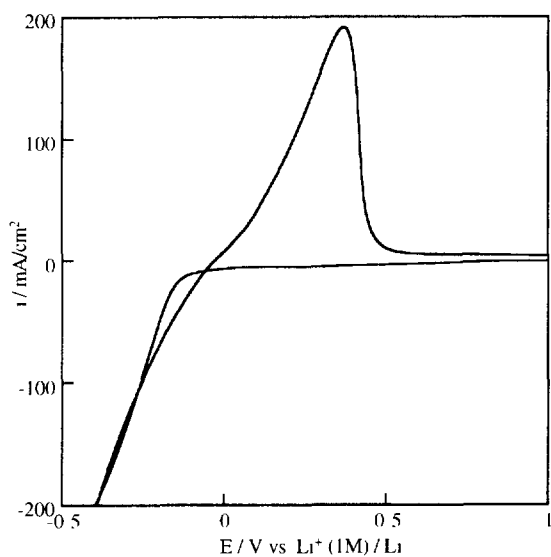

Fig 6 Cyclic voltammogram at the Pt microelectrode (diameter 30 μm) in 8LiClO₄/33PC + 38EC/21PAN (mol%) electrolyte at 21 °C, which was used for the kinetic analysis using Allen–Hickling plot, scan rate: 1 V/s.
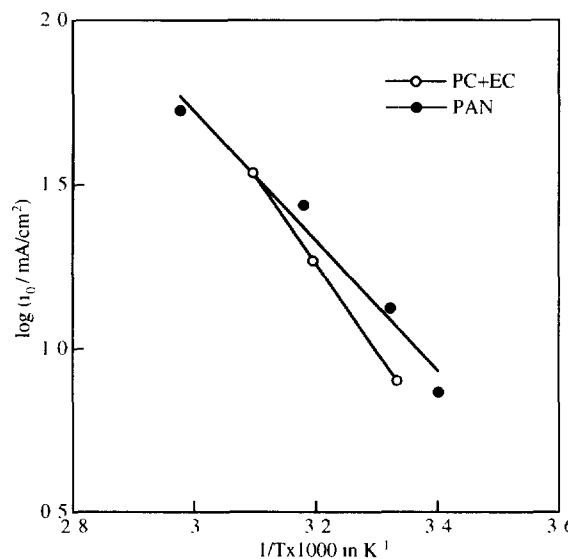

Fig. 8. Arrhenius plot for the exchange current density of Li deposition/dissolution in 1 M LiClO₄/PC + EC solution and 8LiClO₄ (1 M)/33PC + 38EC/21PAN (mol%) electrolyte.

potential at which Li began to deposit was more negative than 0 V, and the current density at the forward scan was lower than that of the backward scan at the more negative potential than 0 V. These results were clearly indicated that Li deposition was in a nucleation process under the activation control, as implied by Pletcher and co-workers in organic solutions [10].

The current density-potential relation for the reversed scan in Fig. 6 was used to construct the Allen–Hickling plot to eliminate the effect of nucleation overpotential, as shown in Fig. 7

$$\log \frac{i}{\exp\left(\frac{nF}{RT}\eta\right) - 1} = \log i_0 - \frac{(1-\alpha)nF}{2.3RT}\eta \qquad (2)$$

where i denotes the current density, R the gas constant, T the absolute temperature, η the overpotential for the Li electrode reaction, i_0 the exchange current density, α the anodic transfer coefficient. The straight lines with the almost same slope were observed at the potential ranging from -0.1 to $+0.3$ V. Table 3 summarizes the values of the exchange current density and the transfer coefficient obtained from the intercept at $\eta = 0$ and slope of the straight line. The exchange current density increased with the temperature as shown in Fig. 8, but the transfer coefficient was almost independent of the temperature and ranged from 0.27 to 0.36. These values were agreed well with that in LiClO₄/PC + EC solution. Again, the plasticized polymer electrolytes behaved as an organic solution of the plasticizer.

Table 3
Kinetic parameters for lithium deposition/dissolution in various plasticized polymer electrolytes together with that in 1 M LiClO$_4$/PC + EC solution

	PC + EC			PAN/PC + EC				PVDF/PC + EC		
	27 °C	40 °C	50 °C	21 °C	28 °C	41.5 °C	63 °C	20 °C	38 °C	70 °C
α	0.34	0.36	0.35	0.26	0.27	0 30	0.31	0.25	0.22	0.30
i_0 (mA/cm^2)	8.0	18.5	34 4	4 1	12 6	26.7	51.7	1.91	2.26	2.99
ΔE_a (kJ/mol)	51.1			37.6				7.5		

In the similar way, the kinetic parameters of Li deposition/dissolution in plasticized PVdF electrolyte were obtained and summarized in Table 3, and found that the exchange current density in PVdF-based electrolyte was smaller than that in PAN-based electrolyte.

4. Conclusions

The microelectrode technique was used to study the Li redox behavior in plasticized polymer electrolytes. The following conclusions were drawn from this work:

1. Conductivities of PAN-, PVC-, PVdF-based plasticized electrolytes were $\sim 10^{-3}$, $\sim 10^{-4}$ and $\sim 10^{-3}$ S/cm at ambient temperature, respectively. These values were almost the same as that in a PC + EC solution.
2. Discontinuity in Arrhenius plots of conductivity and the diffusion coefficient of the Li ion in PAN-based electrolyte was observed, indicating the existence of a low melting point phase in the system.
3. The aggravating effect of the electrolyte decomposition reaction with freshly deposited Li was suppressed at high scan rate or positive reversed potential due to a short exposure duration of Li surface in the electrolyte.
4. Kinetic parameters of Li deposition/dissolution and Li-ion diffusion were evaluated for PAN- and PVdF-based electrolytes, and found that the plasticized polymer electrolytes behaved as a pure organic solution of the plasticizer.

Acknowledgements

References

[1] D.W. Xia, D. Soltz and J. Smid, Solid State Ionics, 14 (1984) 221
[2] K.M. Abraham and M. Alamgir, J. Electrochem. Soc., 137 (1990) 1657
[3] K.M. Abraham and S.B. Brummer, in J.-P Gabano (ed.), Lithium Batteries, Academic Press, New York, 1983, p. 371.
[4] D Aurbach, Y. Ein-Ely and A. Zaban, J Electrochem Soc., 141 (1994) L1.
[5] M. Fleichmann, S. Pons, D R Rolison and P.P. Schmidt, Ultramicroelectrode, Datatech Systems Inc., Morganton, NC, USA, 1987.
[6] X. Wang, T Nishina and I. Uchida, Surf. Technol., 46 (1995) 941 (in Japanese)
[7] M W. Verbrugge and B.J. Koch, J. Electroanal. Chem., 367 (1994) 123.
[8] M W. Verbrugge and B.J Koch, J. Electrochem. Soc., 141 (1994) 3053.
[9] W M Hedges and D. Pletcher, J. Chem. Soc Faraday. Trans 1, 82 (1986) 179
[10] W.M. Hedges, D. Pletcher and C. Gosden, J Electrochem. Soc., 134 (1987) 1334
[11] M Alamgir and K.M. Abraham, J. Electrochem. Soc., 140 (1993) L96.
[12] E Tsuchida, H. Ohno and K. Tsunemi, Electrochim Acta, 28 (1983) 591
[13] X.Q. Yang, H.S. Lee, L Hanson, J. McBreen and Y. Okamoto, J Power Sources, 54 (1995) 198.
[14] A.J. Bard and L.R. Faulkner, Electrochemical Methods, Wiley, Singapore, 1980.
[15] D. Fauteux, Electrochim. Acta, 38 (1993) 1199.